



## Correlation between non- 180 ° domain structures in ( 1 - x ) PbA 1/3 Nb 2/3 O 3 - x PbTiO 3 single crystals ( A = Mg or Zn) under an applied [001] electric field

V. Yu. Topolov, Hu Cao, and D. Viehland

Citation: [Journal of Applied Physics](#) **102**, 024103 (2007); doi: 10.1063/1.2753585

View online: <http://dx.doi.org/10.1063/1.2753585>

View Table of Contents: <http://scitation.aip.org/content/aip/journal/jap/102/2?ver=pdfcov>

Published by the [AIP Publishing](#)

---

### Articles you may be interested in

[Polarization rotation and field induced phase transition in PZN-4.5%PT single crystal](#)

[J. Appl. Phys.](#) **114**, 084109 (2013); 10.1063/1.4819763

[Nanotwin domains in high-strain ferroelectric 89.5 % Pb \( Zn 1 / 3 Nb 2 / 3 \) O 3 - 10.5 % PbTiO 3 single crystal](#)

[J. Appl. Phys.](#) **108**, 106102 (2010); 10.1063/1.3505638

[Correlation between number of ferroelectric variants and coercive field of lead ziconate titanate single crystals](#)

[Appl. Phys. Lett.](#) **91**, 032902 (2007); 10.1063/1.2759274

[Temperature- and electric-field-dependent domain structures and phase transformations in \(001\)-cut tetragonal Pb \( Mg 1/3 Nb 2/3 \) 1 - x Ti x O 3 \( x = 0.40 \) single crystal](#)

[J. Appl. Phys.](#) **97**, 114112 (2005); 10.1063/1.1927288

[X-ray and neutron diffraction investigations of the structural phase transformation sequence under electric field in 0.7 Pb \( Mg 1/3 Nb 2/3 \) - 0.3 PbTiO 3 crystal](#)

[J. Appl. Phys.](#) **96**, 1620 (2004); 10.1063/1.1766087

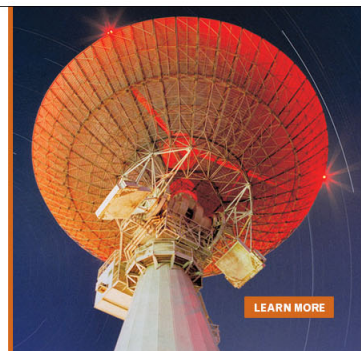
---

MIT LINCOLN  
LABORATORY  
CAREERS

Discover the satisfaction of  
innovation and service  
to the nation

- Space Control
- Air & Missile Defense
- Communications Systems & Cyber Security
- Intelligence, Surveillance and Reconnaissance Systems
- Advanced Electronics
- Tactical Systems
- Homeland Protection
- Air Traffic Control

 **LINCOLN LABORATORY**  
MASSACHUSETTS INSTITUTE OF TECHNOLOGY



LEARN MORE

# Correlation between non-180° domain structures in $(1-x)\text{PbA}_{1/3}\text{Nb}_{2/3}\text{O}_3-x\text{PbTiO}_3$ single crystals (A=Mg or Zn) under an applied [001] electric field

V. Yu. Topolov<sup>a)</sup>

Department of Physics, Southern Federal University, Zorge Street 5, 344090 Rostov-on-Don, Russia

Hu Cao and D. Viehland

Department of Materials Science and Engineering, Virginia Tech, Blacksburg, Virginia 24061

(Received 12 March 2007; accepted 30 May 2007; published online 16 July 2007)

This work is devoted to the study of heterophase states in  $(1-x)\text{PbA}_{1/3}\text{Nb}_{2/3}\text{O}_3-x\text{PbTiO}_3$  or PAN- $x$ PT (A=Mg or Zn) single crystals under an electric field  $E_{\parallel}[001]$ . The possibility of elastically matched phases in the transformational sequences of  $Pm3m \rightarrow P4mm \rightarrow Cm$ ,  $Pm3m \rightarrow Cm$ , and  $P4mm \rightarrow Cm$  are considered with regards to non-180° domains and changes in lattice parameters. Systems of diagrams linking domain types with interfaces between coexisting polydomain phases in PMN-0.28PT and PZN-0.045PT crystals are given. An important role of an intermediate  $P4mm$  phase in achieving stress accommodation has been identified by analysis of lattice parameters of PMN-0.28PT, and the elastic compatibility conditions between non-180° domain structures in the  $P4mm$  and  $Cm$  phases have been determined for various heterophase states. Two scenarios of changes in the lattice parameter  $a_T$  in the  $P4mm$  phase of PMN-0.28PT have first been discussed to reveal possibilities of stress accommodation in heterophase states. It has been shown that the correlation between domain structures in different heterophase states of studied crystals stems from coordinated unit-cell behavior under  $E_{\parallel}[001]$ . © 2007 American Institute of Physics. [DOI: 10.1063/1.2753585]

## I. INTRODUCTION

Perovskite-type relaxor-ferroelectric single crystals of  $(1-x)\text{PbMg}_{1/3}\text{Nb}_{2/3}\text{O}_3-x\text{PbTiO}_3$  (PMN- $x$ PT) and  $(1-x)\text{PbZn}_{1/3}\text{Nb}_{2/3}\text{O}_3-x\text{PbTiO}_3$  (PZN- $x$ PT) are of interest due to their excellent electromechanical properties. Near a morphotropic phase boundary (MPB), these single crystals have high piezoelectric,<sup>1,2</sup> dielectric,<sup>1,2</sup> and electromechanical coupling<sup>1</sup> constants at room temperature and are known to possess various polydomain<sup>3-5</sup> and heterophase<sup>4,6-8</sup> structures. The outstanding properties are related to intermediate monoclinic phases:<sup>6-10</sup> three monoclinic phases— $M_A$ ,  $M_B$ , and  $M_C$  (Ref. 11)—have been reported over various ranges of  $x$ , temperature ( $T$ ), and electric field ( $E$ ) that “bridge” rhombohedral ( $R$ )  $R3m$  and tetragonal ( $T$ )  $P4mm$  ones.<sup>12</sup>

Following a recent report by Cao *et al.*,<sup>13</sup> the  $x$ - $T$  diagram of PMN- $x$ PT ( $0.20 < x < 0.40$ ) for  $E_{\parallel}[001]$  has regions of cubic or  $C$  ( $Pm3m$ ), distorted  $C$ , and three ferroelectric phases— $T$  ( $P4mm$ ),  $M_A$  ( $Cm$ ), and  $M_C$  ( $Pm$ ). The  $T$  phase has been found to be intermediate<sup>13</sup> between the  $C$  and  $M_A/M_C$  ones in the field-cooled (FC) crystal sample. The phase sequence of FC (001) PMN- $x$ PT is  $C \rightarrow M_A$  for  $x < 0.25$ ,  $C \rightarrow T \rightarrow M_A$  for  $0.25 \leq x \leq 0.30$ ,  $C \rightarrow T \rightarrow M_C$  for  $0.30 \leq x \leq 0.35$ , and  $C \rightarrow T$  for  $x > 0.35$ : please note that the stability of the intermediate  $T$  phase extends<sup>14</sup> from  $x=0.30$  in the zero-field-cooled (ZFC) state to  $x=0.25$  in the FC state. Subsequently, studies of different orientations revealed a “fragile” phase stability that was different along different crystallographic zones. For  $x=0.30$ , the following sequences

were observed on field cooling:  $C \rightarrow T \rightarrow M_C \rightarrow M_A$  for  $E_{\parallel}[001]$  (Ref. 15) and  $C \rightarrow T \rightarrow \text{orthorhombic} \rightarrow M_B$  for  $E_{\parallel}[110]$  (Ref. 2) or  $E_{\parallel}[111]$  (Ref. 16). The transformational sequence of PZN- $x$ PT is similar to that of PMN- $x$ PT,<sup>2,13-17</sup> except for one notable difference. This is at room temperature with increasing  $E_{\parallel}[001]$  that the  $T$  phase in PZN- $x$ PT can be induced from the  $M_A$  one at lower PT contents than that in PMN- $x$ PT,<sup>18</sup> that is for compositions of equal distances from their corresponding MPBs.

It is known that both the phase stability and physical properties of FC PMN- $x$ PT single crystals are dramatically different<sup>2,14,15,17</sup> than those of the ZFC. The remarkable properties of the monoclinic phases observed in these single crystals have been attributed to adaptive phases formed by nanosized domains of the  $T$  phase and treated in analogy to adaptive martensite.<sup>19</sup> General invariance conditions that achieve stress accommodation by apparent changes in crystal lattice parameters were shown to be fulfilled for PMN- $x$ PT and PZN- $x$ PT compositions located near the MPB. The self-adjusting lattice parameters of this adaptive phase are the consequence of elastic compatibility of a coherent mixture of these nanosized ferroelectric domains.<sup>19</sup>

In contrast, here, we consider how changes in the crystal lattice parameters of coexisting ferroelectric phases can result in a metastable heterophase state. We do not consider the case of conformal domain miniaturization, but rather that of coexisting micron-sized domains of different point group symmetries. Systems of diagrams linking domain types with interfaces between coexisting phases are identified on the basis of stress accommodation and the elastic compatibility

<sup>a)</sup>Electronic mail: topolov@phys.rsu.ru

conditions. We then show a correlation between domain (twin) structures and interfaces between the coexisting  $T$  and  $M_A$  phases in PMN-0.28PT and PZN-0.045PT crystals for  $E \parallel [001]$ .

## II. ELASTICALLY MATCHED POLYDOMAIN PHASES AND DOMAIN ORIENTATIONS THEREOF

Formation of domain (twin) structures in ferroelectric and related single crystals has previously been described in terms of thermodynamic<sup>20</sup> and crystallographic<sup>21</sup> theories. It is known that a lowering of the energy of an internal mechanical stress field, associated with changes in lattice parameters and phase coexistence, can result in the formation of equilibrium (structural or elastic) domain structures.<sup>20</sup> Newly transformed polydomain phases can then coexist with the parent phase, where their interfaces are planar and undistorted on average. As shown by Roytburd,<sup>20</sup> the domains of coexisting phases may act as elastic domains, vanishing their excess elastic energy. A crystallographic interpretation of heterophase states that appear at martensite phase transitions in the presence of elastic domains was previously proposed.<sup>22,23</sup> To name an example, a crystallographic description of two polydomain ferroelectric phases (in terms of their distortions) has been put forward,<sup>24</sup> where conditions for complete stress relaxation along the interfaces were formulated. In this case, Metrat's concepts<sup>24</sup> were modified and subsequently applied<sup>25</sup> to polydomain phases belonging to different symmetry groups or regions with complicated domain (twin) structures.

In our present study, we assume that a mechanically free crystal undergoes a first-order phase transition in certain temperature  $T$  and electric field  $E$  ranges. The axes of the rectangular coordinate system ( $X_1X_2X_3$ ) are oriented parallel to the crystallographic axes of the perovskite unit cell in the  $C$  phase (i.e.,  $OX_1 \parallel [100]$ ,  $OX_2 \parallel [010]$ , and  $OX_3 \parallel [001]$ ). Possible orientations of non-180° elastic twin domains formed under  $E \parallel [001]$  are represented in Fig. 1 for (a) the tetragonal  $T$  and (b) monoclinic  $M_A$  phases. The lamellar domain structures previously reported<sup>5</sup> in PMN- $x$ PT and PZN- $x$ PT crystals are assumed to contain stress-free domain walls oriented<sup>26</sup> along the  $\{110\}$ -type planes (i.e., in the  $T$  phase) or  $\{100\}$ -type planes (i.e., in the  $M_A$  phase). The distortion  $3 \times 3$  matrices of the polydomain  $T$  and  $M_A$  phases— $\|N_T(n_T)\|$  and  $\|N_{MA}(f_{MA}, v_{MA})\|$ , respectively—can be written in terms of the unit-cell distortions<sup>6</sup> and volume fractions of individual domain types ( $T$  phase) or twins ( $M_A$  phase). In the distortion matrices  $n_T$  denotes the volume fraction of the domains with  $P_{T,1} \parallel [001]$  in the  $T$  phase [Fig. 1(a)] and  $f_{MA}$  and  $v_{MA}$  characterize the volume fractions of the domains in the  $M_A$  phase [Fig. 1(b)]. The distortion matrix  $\|N_C\|$  of the  $C$  phase is the identity  $3 \times 3$  matrix.

To obtain a more detailed analysis of the elastic matching of the coexisting phases, the distortion matrices of the phases need to be taken in pairs and simultaneously substituted into formulas to solve by an algorithm.<sup>6</sup> In the general case, interfaces between coexisting phases 1 (distortion matrix  $\|N^{(1)}\|$ ) and 2 (distortion matrix  $\|N^{(2)}\|$ ) can be characterized as quadric surfaces: such surfaces are described by an

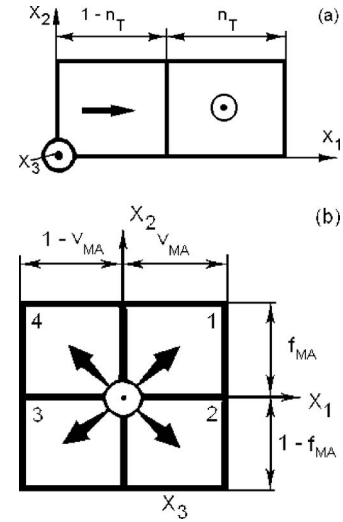


FIG. 1. Schematic illustration of non-180° domains in ferroelectric (a) tetragonal  $T$  and (b) monoclinic  $M_A$  phases of PMN- $x$ PT and PZN- $x$ PT single crystals for  $E \parallel [001]$ . The domains in the  $T$  phase are characterized by spontaneous polarization vectors  $P_{T,1} \parallel [001]$  (volume fraction  $n_T$ ) and  $P_{T,2} \parallel [100]$  (volume fraction  $1-n_T$ ), as shown in (a). The domains in the  $M_A$  phase are characterized by spontaneous polarization vectors  $P_{Ma,1} \parallel [dd1]$  (volume fraction  $f_{MA}v_{MA}$ ),  $P_{Ma,2} \parallel [dd\bar{1}]$  [volume fraction  $(1-f_{MA})v_{MA}$ ],  $P_{Ma,3} \parallel [d\bar{d}1]$  [volume fraction  $(1-f_{MA})(1-v_{MA})$ ], and  $P_{Ma,4} \parallel [d\bar{d}\bar{1}]$  [volume fraction  $f_{MA}(1-v_{MA})$ ], as shown in (b). The axes  $OX_j$  of the Cartesian coordinate system ( $X_1X_2X_3$ ) were fixed as follows:  $OX_1 \parallel [100]$ ,  $OX_2 \parallel [010]$ , and  $OX_3 \parallel [001]$ .

equation  $\sum_{a,b=1}^3 D_{ab} x_a x_b = 0$ , when referenced to the coordinate system ( $X_1X_2X_3$ ). The coefficients  $D_{ab} = \sum_{f=1}^3 (N_{af}^{(2)} N_{bf}^{(2)} - N_{af}^{(1)} N_{bf}^{(1)})$  are written in terms of the elements of the  $\|N^{(1)}\|$  and  $\|N^{(2)}\|$  matrices, which depend on the volume fractions of the different types of non-180° domains in phases 1 and 2, respectively. The geometry of the interfaces between phases 1 and 2 then depends on the signs of invariant conditions,<sup>6,8</sup> which can be given as

$$I = D_{11} + D_{22} + D_{33}, \quad D = \det \|D_{ab}\|,$$

$$\text{and } J = \begin{vmatrix} D_{11} & D_{12} \\ D_{21} & D_{22} \end{vmatrix} + \begin{vmatrix} D_{22} & D_{23} \\ D_{32} & D_{33} \end{vmatrix} + \begin{vmatrix} D_{33} & D_{31} \\ D_{13} & D_{11} \end{vmatrix}. \quad (1)$$

From these matrices characterizing the aforementioned quadric surfaces, we can identify three distinct real conical regions: I, II, and III. These regions are described by the following pairs of inequalities:  $DI < 0$  and  $J < 0$  (region I),  $DI < 0$  and  $J > 0$  (region II), and  $DI > 0$  and  $J < 0$  (region III). The orientation of the conical interfaces with respect to the perovskite unit-cell axes depends on the balance of the  $D_{ab}$  coefficients. In one particular case,<sup>27</sup> the cross section of the interface by the (001) plane consisted of a pair of intersecting lines  $x'_2 = \pm f x'_1$ , where  $f = [-(D_{11} \cos^2 \alpha + D_{12} \sin 2\alpha + D_{22} \sin^2 \alpha) / (D_{11} \sin^2 \alpha - D_{12} \sin 2\alpha + D_{22} \cos^2 \alpha)]^{1/2}$ , where the  $OX'_j$  axes are connected with the  $OX_j$  ones ( $j=1$  and 2) by a counter-clockwise rotation with respect to  $OX_3$ , and where the rotation angle is  $\alpha = 0.5 \tan^{-1}[2D_{12}/(D_{11} - D_{22})]$ . It can also be seen that the cross-section characteristics depend on  $D_{kl}$  with  $k, l=1$  and 2 only. For comparison, it should be mentioned that various conical surfaces predicted within the framework of the invariants (1) were first visualized<sup>27</sup> in PbZrO<sub>3</sub> single crystals undergoing a first-

order  $C-R$  phase transition. Moreover, a mutual arrangement of the aforementioned intersecting lines and an orientation of an internal bisectrix therein were in agreement with experimental crystallographic characteristics of the conical interfaces for  $\text{PbZrO}_3$ .<sup>27</sup> A bending of these interfaces was observed in these crystals, wherein conditions for complete stress relaxation were unfavorable at the  $C-R$  phase transition due to equal diagonal distortions<sup>25,27</sup> of the non-180° domains in the  $R$  phase.

As follows from our results, the coefficients  $D_{ab}$  from Eqs. (1) are regarded as polynomials of  $n_T$ ,  $f_{MA}$ , and  $v_{MA}$  (up to sixth order in these parameters). This does not enable one to obtain the invariants (1) in an explicit form even for a concrete heterophase state consisting of two polydomain phases with two domain types in each phase. Along with the aforementioned regions I–III, there is also a fourth region (IV), however, it is related to an imaginary conical apex described by the inequalities  $DI > 0$  and  $J > 0$ . This geometrical feature suggests that it becomes impossible to find proper conditions for stress accommodation at quadric interfaces in heterophase single crystals; accordingly, other ways for achieving stress accommodation are necessary, such as forming zig-zag interfaces or transition regions close to the interfaces.

The elastic matching in the heterophase structure that gives zero net strain planes (ZNSPs)<sup>4,6,8,10</sup> obeys the following compatibility conditions:

$$DI = 0, \quad J < 0. \quad (2)$$

These compatibility conditions must hold true on each and every boundary separating regions I and III. The conditions (2) dictate the planar interfaces that are capable of providing complete stress accommodation in the crystal, vanishing the excess elastic energy due to the heterophase state. We next solve these conditions (1) and (2) by an algorithm, summarizing various interfaces and domain types in diagrams of heterophase states under  $E \parallel [001]$ . In this study, we did not consider the additional effect of dislocations or of an imperfect matching of the phases along interfaces.

### III. DIAGRAMS OF DOMAIN TYPES AND INTERFACES IN HETEROPHASE SINGLE CRYSTALS

Recently, Wang<sup>28</sup> carried out a systematic analysis of the lattice parameters and their changes at the  $T-M_C$  phase transition in  $\text{PMN-xPT}$  and  $\text{PZN-xPT}$  compositions near the MPB. This approach was based on three intrinsic relationships previously derived assuming an adaptive ferroelectric phase transformation:<sup>19</sup> there the lattice parameters of the intermediate  $M_C$  phase were related to those of the  $T$  and  $C$  ones. Here, we now consider features of the elastic matching of the coexisting phases (i.e.,  $C-T$ ,  $T-M_A$ , and  $C-M_A$ ), and put forward a series of diagrams that summarize the possible domain types and interfaces for different heterophase structures that can be stable under  $E \parallel [001]$ . We calculated these diagrams by (1) and (2), using as input experimental lattice parameter data for FC  $\text{PMN-xPT}$  ( $x=0.24$  and  $0.28$ ) (Ref. 13) and for  $\text{PZN-0.045}$  crystals<sup>18</sup> undergoing an electric-field induced  $T \rightarrow M_A$  phase transition at room temperature.

Due to a lack of experimental data on the monoclinic angle  $\beta_{MA}(T)$  or the shear angle  $\omega_{MA}(T) = 90^\circ - \beta_{MA}(T)$  as a function of temperature in the  $M_A$  phase of  $\text{PMN-xPT}$ ,<sup>13</sup> the values of  $\omega_{MA}$  were taken to be in a range of  $0.04^\circ - 0.10^\circ$ . These values are consistent with those measured<sup>14,15</sup> at fixed temperature  $T$  and field  $E$ .

#### A. Polydomain/heterophase $\text{PMN-xPT}$ ( $x=0.28, 0.27$ , and $0.24$ )

Jumps in lattice parameters<sup>13</sup> at the  $C-T$  phase transition in  $\text{PMN-0.28PT}$  ( $T_C \approx 382$  K,  $E \parallel [001]$ , and  $E=0.5$  kV/cm) promote the formation of ZNSPs along the interfaces between the two phases. As a consequence, the  $T$  phase splits into  $90^\circ$  domains that are illustrated in Fig. 1(a), with optimal volume fractions  $n_T^{\text{opt}}$  and  $1 - n_T^{\text{opt}}$ , where  $n_T^{\text{opt}} = 0.545$ . The  $n_T^{\text{opt}}$  value is approximately equal to that recently reported<sup>30</sup> for related FC  $\text{PMN-xPT}$  ( $x=0.30$  or  $0.32$ ) crystals. Please note in the present case and this prior one that  $n_T^{\text{opt}} \approx 1/2$  and that the lattice parameters of the coexisting  $C$  ( $a_C$ ) and  $T$  ( $a_T$  and  $c_T$ ) phases obey the equality  $c_T - a_C \approx a_C - a_T$ . However, due to the fact that  $E \parallel [001]$ , the value of  $n_T$  whose domains have its polarization oriented in the direction of the applied field [ $P_T \parallel E$ , see Fig. 1(a)] is expected to be slightly greater than  $1/2$ .

On field-cooling ( $E=0.5$  kV/cm), the  $T$  phase of (001)  $\text{PMN-0.28PT}$  transforms to  $M_A$  over a temperature transition window of about 10 K. The temperature dependence of  $a_T$  and  $c_T$  in this transition window of about 382–362 K was continuous with that in the  $C$  phase. However, on cooling ( $E=0.5$  kV/cm) between 362 and 358 K,  $a_T$  exhibited a jump in value<sup>13</sup> of  $|a_T(358 \text{ K}) - a_T(362 \text{ K})|/a_T(362 \text{ K}) \approx 0.06\%$ , whereas  $c_T(T)$  exhibited only a slight continuous decrease. However, under a lower field of 0.25 kV/cm, FC (001)  $\text{PMN-0.28PT}$  did not exhibit any anomaly in  $a_T$  over the same vicinity of the  $T-M_A$  phase transition.<sup>14</sup> Changes in the lattice parameter  $a_T$  can influence the coexistence of  $T$  and  $M_A$  phases, via relaxation of the excess elastic energy by achieving elastic compatibility. Accordingly, the difference in lattice parameters for  $\text{PMN-0.28PT}$  cooled under different electric fields can affect the metastable two phase  $T-M_A$  equilibrium. Thus, we consider the two different scenarios described later.

In the first scenario, we used the lattice parameters<sup>13</sup> of the  $T$  phase at  $T_I = 358$  K and of the  $M_A$  phase at  $T_{II} = 356$  K, and evaluated invariants (1) for the domain types given in Fig. 1. This resulted in unfavorable conditions for forming ZNSPs in heterophase  $\text{PMN-0.28PT}$  crystals. The interfaces between polydomain  $T$  and  $M_A$  phases would be ZNSPs at fairly small  $n_T$  values ( $0 \leq n_T \leq 0.260$ ); however, cooling under  $E \parallel [001]$  promoted  $n_T$  to be greater than  $1/2$ . For  $n_T > 1/2$ , there were no  $f_{MA}$  and  $v_{MA}$  values that satisfy the conditions given in Eq. (2); consequently, relaxation of the mechanical stress was problematic. It should also be mentioned that regions of polydomain  $T$  phase in the temperature range of 362–358 K cannot be separated by ZNSPs, due to the aforementioned jump in  $a_T$  that results in an inequality  $|a_T(358 \text{ K}) - a_T(362 \text{ K})|/a_T(362 \text{ K}) \gg |c_T(358 \text{ K}) - c_T(362 \text{ K})|/c_T(362 \text{ K})$ . The lack of ZNSPs between elas-

tically matched polydomain  $T$  phase regions would also increase  $T_I$  toward that of  $T_C=382$  K. Moreover, elastic clamping in a bulk crystal sample may result in the formation of a new low-symmetry phase, inducing additional structural phase transitions providing the conditions for further stress relaxation. Details for such behavior in ferroelectric and related single crystals (in the presence of the internal stress fields) were considered previously by Pertsev and Salje.<sup>29</sup>

In the second scenario, we used the experimental lattice parameters at 362 and 356 K. These lattice parameters are accurate to within 2% of measured ones<sup>14</sup> for PMN-0.28PT crystals at the  $T-M_A$  phase transition under  $E=0.25$  kV/cm. Upon using these values, we obtained favorable conditions for forming ZNSPs. According to our calculations,  $T-M_A$  interfaces oriented along the ZNSPs would appear for  $0.648 \leq n_T \leq 0.991$ , with  $0.103 \leq n_T - n_T^{\text{opt}} \leq 0.446$ . This implies that slight changes in the domain structure of Fig. 1 caused by  $90^\circ$  domain-wall displacements under  $E \parallel [001]$  would promote effective stress relaxation, allowing for stable heterophase states.

We summarize our findings in diagrams (Fig. 2) for polydomain heterophase states in PMN-0.28PT, following the second scenario of lattice parameter changes. These diagrams are given in Fig. 2 for the following volume fractions of the  $90^\circ$  domains with  $P_T \parallel [001]$ : (a)  $n_T=0.65$ , (b)  $n_T=0.80$ , and (c)  $n_T=0.95$ . The results show that conditions (2) hold, and non- $180^\circ$  domain structures of the  $T$  and  $M_A$  phases can coexist over wide ranges of  $n_T$ ,  $f_{MA}$ , and  $v_{MA}$ . However, for  $n_T \rightarrow 1$ , our results show a shift in the ZNSP boundaries [see Figs. 2(b) and 2(c)] that favors the stability of a single-domain  $M_A$  state.

Certain tendencies toward stress relaxation were also revealed for PMN-0.27PT, where the phase sequence  $C \rightarrow T \rightarrow M_A$  is observed for  $E \parallel [001]$ . Based on experimental data,<sup>14</sup> we obtained  $n_T^{\text{opt}}=0.675$  for the  $C-T$  transition. Diagrams for the  $T-M_A$  interfaces and related heterophase domain states are similar to those given in Fig. 2, and thus are not shown. These interfaces are ZNSPs for  $0 \leq n_T \leq 0.930$ ; and therefore, no additional  $90^\circ$  domain-wall displacements are required. The similarity between the diagrams for PMN-0.28PT (second scenario) and PMN-0.27PT was due to analogous interrelations between lattice parameters of the  $T$  and  $M_A$  phases:  $b_{MA} - a_T < c_T - c_{MA} < a_{MA} - a_T$ . However, for PMN-0.28PT, the lattice parameters from the first scenario do not obey this condition, owing to a decrease in the difference  $a_{MA} - a_T$  after taking into account the earlier-described jump in  $a_T$ .

Contrary to PMN-0.28PT, the lattice parameter changes in the vicinity of the  $C-M_A$  phase transition<sup>13</sup> for PMN-0.24PT do not allow for the formation of ZNSPs and for the stress relaxation required for stable heterophase states to exist. For each pair  $(f_{MA}, v_{MA})$  from ranges of  $0 \leq f_{MA} \leq 1$  and  $0 \leq v_{MA} \leq 1$ , our calculations revealed that the interfaces between  $C$  and polydomain  $M_A$  phases are conical: all pairs  $(f_{MA}, v_{MA})$  in this diagram are related to region III only.

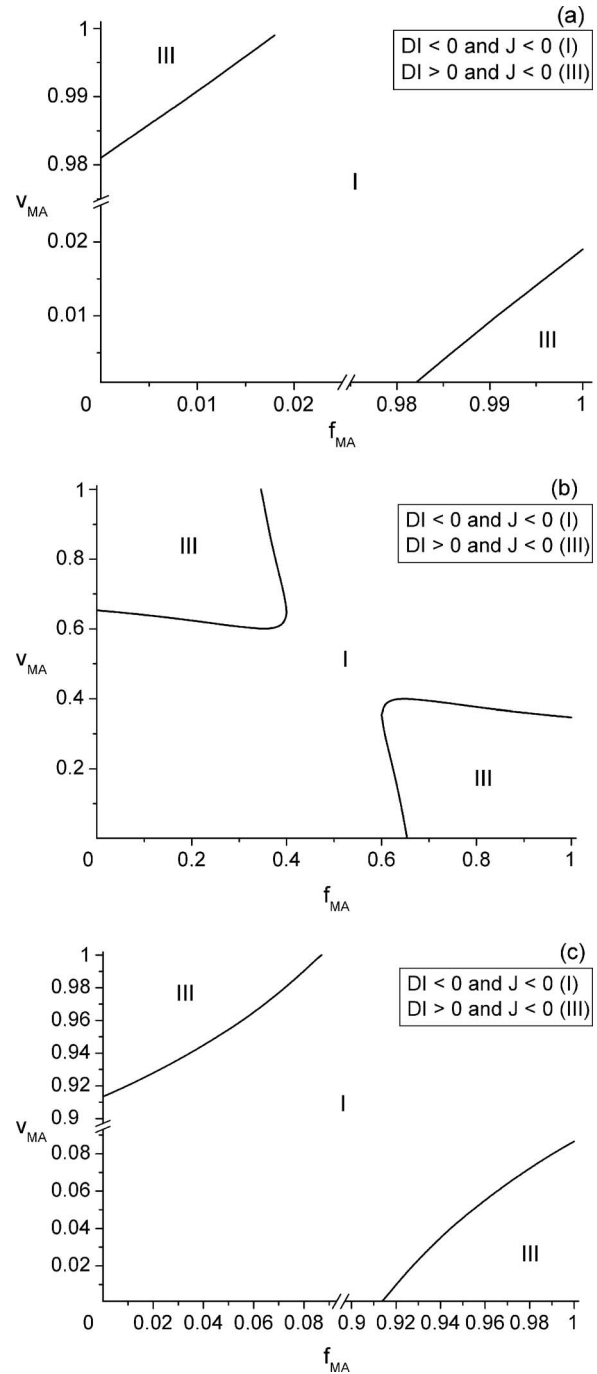


FIG. 2. Diagrams of heterophase domain types and interfaces at the  $T-M_A$  transition in FC PMN-0.28PT crystals with a field of 0.5 kV/cm applied parallel to  $[001]$  for (a)  $n_T=0.65$ , (b)  $n_T=0.80$ , and (c)  $n_T=0.95$ . The parameters  $n_T$ ,  $f_{MA}$ , and  $v_{MA}$  which describe volume fractions of different domain types are defined in Fig. 1. The boundaries between regions I and III correspond to ZNSPs.

These features of region III associated with lattice parameters jumps<sup>13</sup> in FC PMN-0.24PT are not required to follow conditions (1) and (2) for existence of ZNSPs. Possibly, the distorted  $C$  phase that exists over a narrow temperature range between the  $C$  and  $M_A$  ones (as shown in the  $x-T$  diagram)<sup>13</sup> could promote stress relaxation: either by changes in the balance of diagonal distortions or by forming a metastable three-phase equilibrium between  $C$ , distorted  $C$ , and  $M_A$  phases. However, this problem is independent of the ap-

proach we summarize in Fig. 2, although it might be interesting to consider as a special scenario in detail at a latter time.

Finally, we varied the shear angle  $\omega_{MA}$  of the perovskite unit cell over the range of  $0.04^\circ$ – $0.10^\circ$ . However, this resulted in small changes ( $<3\%$ ) in  $(f_{MA}, v_{MA})$  values related to the ZNSPs in the diagrams given in Fig. 2. Moreover, ZNSPs were not predicted to appear at the  $C$ – $M_A$  phase transition in PMN–0.24PT as a consequence of varying  $\omega_{MA}$ .

## B. Polydomain/heterophase PZN–0.045PT

The  $T$ – $M_A$  phase transition in PZN–0.045PT occurs with increasing field near  $E \approx 11$  kV/cm at room temperature.<sup>18</sup> It is reasonable to assume that the  $T$  phase being stable at higher fields is either a single-domain state or splits into  $90^\circ$  polydomains with a significant prevalence for variants having their spontaneous polarization vectors  $P_{T, \parallel E} \parallel [001]$  [Fig. 1(a)]. We designate this prevalent variant as that with volume fraction  $n_T$ . Figure 3 shows the summary of diagrams for (a)  $n_T=0.90$ , (b)  $n_T=0.95$ , and (c)  $n_T=0.99$ . The diagrams show that as  $n_T \rightarrow 1$  that ZNSPs appear only in narrow ranges of  $(f_{MA}, v_{MA})$ . For lower values of  $n_T$ , the  $M_A$  phase is split into polydomains; however, with increasing  $n_T$ , there is a distinct prevalence of one domain type over others, in particular over the range of  $0.95 < n_T < 1$  [compare Figs. 3(b) and 3(c)]. The largest volume fraction of the domains in the  $M_A$  phase are those with  $P_{MA, 2}$  or  $P_{MA, 4}$  [Fig. 1(b)], as described by conditions

$$f_{MA} \rightarrow 0 \text{ and } v_{MA} \rightarrow 1; \quad f_{MA} \rightarrow 1 \text{ and } v_{MA} \rightarrow 0, \quad (3)$$

respectively. The possibility of the coexistence of single-domain  $T$  and  $M_A$  phases is energetically close to the required conditions (1) and (2) for ZNSPs:<sup>22</sup> according to these conditions, relationships between diagonal elements of distortion matrices  $\|N_T\|$  and  $\|N_A\|$  can be given as

$$N_{T,11} < N_{MA,11}, \quad N_{T,22} = N_{MA,22}, \quad N_{T,33} > N_{MA,33}. \quad (4)$$

Relationships (4) are in agreement with conditions of the perovskite lattice parameters  $(a_T, c_T)$  and  $(a_{MA}, b_{MA}, c_{MA})$  for coexisting phases. At the  $T$ – $M_A$  phase transition in PZN–0.045PT, these conditions are

$$a_T < a_{MA}, \quad a_T = b_{MA}, \quad c_T > c_{MA}. \quad (5)$$

Please note that the monoclinic distortion ( $\omega_{MA} \neq 0$ ) can slightly affect the domain (twin) structure of the  $M_A$  phase, but cannot violate the balance of the diagonal elements given by formulas (4).

It should be mentioned for comparisons that the coexistence of two untwined phases is to this date unique to a prior study of PbHfO<sub>3</sub> crystals,<sup>31</sup> in which antiferroelectric  $P222_1$  and  $Pba2$  phases are separated by a ZNSP interface at  $E = 0$ . However, contrary to conditions (5), the perovskite lattice parameter  $b$  of PbHfO<sub>3</sub> undergoes a jump at a first-order  $P222_1 \rightarrow Pba2$  transition.

## IV. CONCLUSION

The features of the elastically matched polydomain (twinned) coexisting  $T$  and  $M_A$  phases have been determined

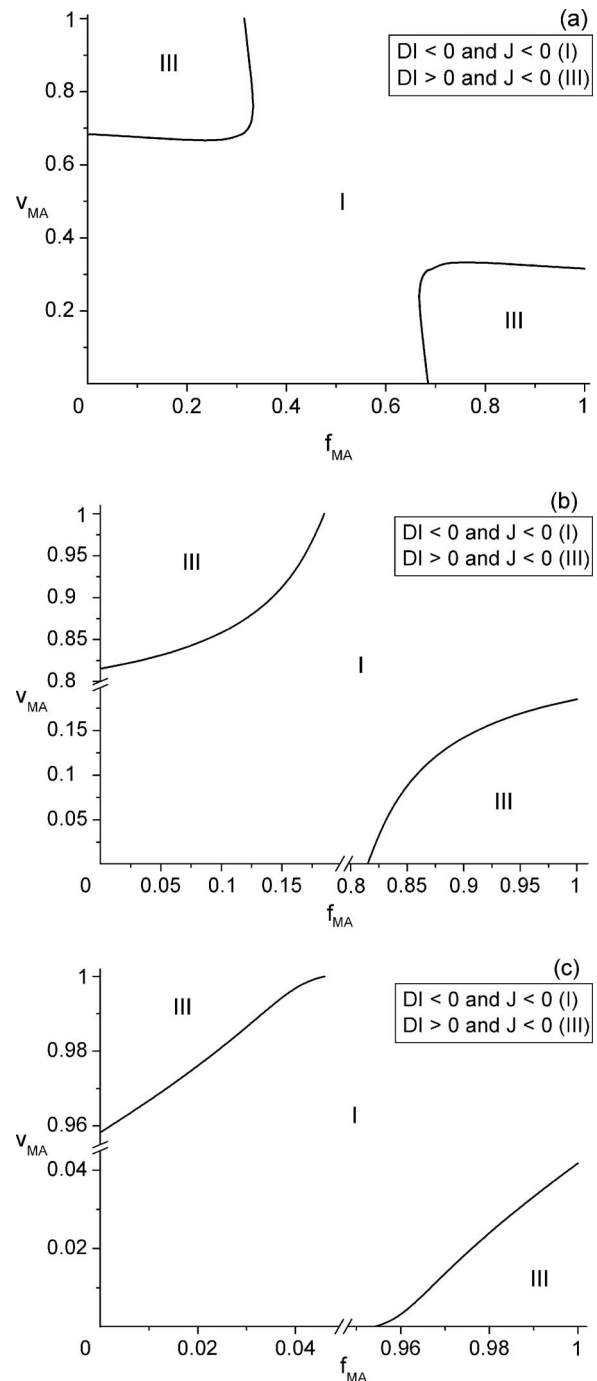


FIG. 3. Diagrams of heterophase domain types and interfaces at the field-induced  $T$ – $M_A$  phase transition in PZN–0.045PT crystals with  $E \parallel [001]$  for (a)  $n_T=0.90$ , (b)  $n_T=0.95$ , and (c)  $n_T=0.99$ .

in PMN–0.28PT and PZN–0.045PT crystals at first-order phase transitions under electric field. For an applied  $E \parallel [001]$ , we have found  $T$ – $M_A$  interfaces and corresponding non- $180^\circ$  domain structures. These domain structures promote phase coexistence via complete stress accommodation that achieves elastic compatibility at planar interfaces (i.e., the ZNSPs). The relationships between possible ZNSPs and the related non- $180^\circ$  domain structures in the  $T$  and  $M_A$  phases were then summarized by systems of diagrams for FC PMN–0.28PT (Fig. 2) and PZN–0.045PT (Fig. 3). Generic tendencies in these diagrams were apparent, enabling us to

conclude a correlation between metastable heterophase domain structures and the volume fractions of some domain types (see Fig. 1) over wide ranges of  $x$ ,  $E$ , and  $T$ . This correlation stems from coordinated unit-cell behavior beginning with lattice parameter adaptations at the  $C$ - $T$  phase transition: it is valid when  $E$  is modest,<sup>13,14</sup> making it possible to consider a restricted number of domain types in the  $T$  and  $M_A$  phases.

Our results show that the  $T$  phase plays an important role as an intermediate phase in PMN-0.28PT. The conditions for achieving complete stress accommodation are strongly dependent on the lattice parameter  $a_T(T)$ , in particular in the vicinity of the  $T$ - $M_A$  transition, and to a lesser extent in PMN-0.27PT. The lack of an intermediate  $T$  phase in the transformational sequence of FC PMN-0.24PT, and the subsequent failing of the  $C$ - $M_A$  interfaces to be ZNSPs results in the development of inhomogeneous internal stress fields inside of the crystal. We hope that our heterophase model and domain stability diagrams for elastically matched polydomain phases will stimulate new studies of phase transformational sequences in perovskite-type solid solutions. It offers an approach to understand how a metastable two-phase field can be stabilized by elastic interactions between domains and to how this metastability can be altered by changes in domain configurations with crystal history and by changes in parameters such as  $x$ ,  $E$ , and  $T$ .

## ACKNOWLEDGMENTS

The authors would like to thank Professor Z.-G. Ye (Canada), Professor A. V. Turik, and Professor V. G. Gavrilyachenko (Russia) for many helpful discussions. This work was partially supported by the administration of the Rostov State University (Southern Federal University since 2007, Project No. 11.1.06f on basic researches), and it is gratefully acknowledged by one of the authors (V.Y.T). Two of the authors (H.C. and D.V.) gratefully acknowledge the support of the Office of Naval Research (USA).

<sup>1</sup>H. Cao, V. H. Schmidt, R. Zhang, W. Cao, and H. Luo, *J. Appl. Phys.* **96**, 549 (2004); R. Zhang, B. Jiang, W. Cao, and A. Amin, *J. Mater. Sci. Lett.* **21**, 1877 (2002).

<sup>2</sup>H. Cao, F. Bai, N. Wang, J. Li, D. Viehland, G. Xu, and G. Shirane, *Phys. Rev. B* **72**, 064104 (2005).

<sup>3</sup>F. Bai, J. Li, and D. Viehland, *Appl. Phys. Lett.* **85**, 2313 (2004); V. V. Shvartsman and A. L. Kholkin, *Phys. Rev. B* **69**, 014102 (2004); V. A. Shuvaeva, A. M. Glazer, and D. Zekria, *J. Phys.: Condens. Matter* **17**,

5709 (2005).

<sup>4</sup>Z.-G. Ye and V. Yu. Topolov, *Ferroelectrics* **253**, 79 (2001); V. Yu. Topolov and Z.-G. Ye, *ibid.* **253**, 71 (2001).

<sup>5</sup>M. Abplanalp, D. Barošová, P. Bridenbaugh, J. Erhart, J. Fousek, P. Günter, J. Nosek, and M. Šulc, *J. Appl. Phys.* **91**, 3797 (2002); A.-É. Renault, H. Dammak, G. Calvarin, M. P. Thi, and P. Gaucher, *Jpn. J. Appl. Phys., Part 1* **41**, 3846 (2002).

<sup>6</sup>V. Yu. Topolov and Z.-G. Ye, *Phys. Rev. B* **70**, 094113 (2004); V. Yu. Topolov, *Phys. Rev. B* **71**, 134103 (2005).

<sup>7</sup>V. Yu. Topolov, *J. Phys.: Condens. Matter* **16**, 2455 (2004); R. Bertram, G. Reck, and R. Uecker, *J. Cryst. Growth* **253**, 212 (2003).

<sup>8</sup>V. Yu. Topolov, *Appl. Phys. Lett.* **89**, 082904 (2006).

<sup>9</sup>B. Noheda, *Curr. Opin. Solid State Mater. Sci.* **6**, 27 (2002).

<sup>10</sup>V. Yu. Topolov and A. V. Turik, *Fiz. Tverd. Tela (Leningrad)* **44**, 1295 (2002); V. Yu. Topolov and A. V. Turik, *Phys. Solid State* **44**, 1355 (2002).

<sup>11</sup>D. Vanderbilt and M. H. Cohen, *Phys. Rev. B* **63**, 094108 (2001).

<sup>12</sup>D. La-Orautapong, B. Noheda, Z.-G. Ye, P. M. Gehring, J. Toulouse, D. E. Cox, and G. Shirane, *Phys. Rev. B* **65**, 144101 (2002); B. Noheda, D. E. Cox, G. Shirane, J. Gao, and Z.-G. Ye, *Phys. Rev. B* **66**, 054104 (2002).

<sup>13</sup>H. Cao, J. Li, and D. Viehland, *J. Appl. Phys.* **100**, 034110 (2006).

<sup>14</sup>H. Cao, J. Li, D. Viehland, and G. Xu, *Phys. Rev. B* **73**, 184110 (2006).

<sup>15</sup>F. Bai, N. Wang, J. Li, D. Viehland, P. M. Gehring, G. Xu, and G. Shirane, *J. Appl. Phys.* **96**, 1620 (2004).

<sup>16</sup>H. Cao, J. Li, and D. Viehland, *J. Appl. Phys.* **100**, 084102 (2006).

<sup>17</sup>H. Cao, F. Bai, J. Li, D. Viehland, G. Xu, H. Hiraka, and G. Shirane, *J. Appl. Phys.* **97**, 094101 (2005); H. Cao, J. Li, D. Viehland, G. Xu, and G. Shirane, *Appl. Phys. Lett.* **88**, 072915 (2006).

<sup>18</sup>B. Noheda, Z. Zhong, D. E. Cox, G. Shirane, S.-E. Park, and P. Rehrig, *Phys. Rev. B* **65**, 224101 (2002).

<sup>19</sup>Y. M. Jin, Y. U. Wang, A. G. Khachatryan, J. F. Li, and D. Viehland, *J. Appl. Phys.* **94**, 3629 (2003); Y. M. Jin, Y. U. Wang, A. G. Khachatryan, J. F. Li, and D. Viehland, *Phys. Rev. Lett.* **91**, 179601 (2003); D. Viehland, *J. Appl. Phys.* **88**, 4794 (2000).

<sup>20</sup>A. L. Roitburd, *Phase Transitions* **45**, 1 (1993); A. L. Roitburd, *Mater. Sci. Eng., A* **127**, 229 (1990).

<sup>21</sup>S. Mendelson, *Ferroelectrics* **37**, 519 (1981).

<sup>22</sup>M. S. Wechsler, D. S. Lieberman, and T. A. Read, *J. Met.* **197**, 1503 (1953); D. S. Lieberman, M. S. Wechsler, and T. A. Read, *J. Appl. Phys.* **26**, 473 (1955).

<sup>23</sup>C. Boulesteix, B. Yangui, M. Ben Salem, C. Manolikas, and S. Amelinckx, *J. Phys. (France)* **47**, 461 (1986).

<sup>24</sup>G. Metrat, *Ferroelectrics* **26**, 801 (1980).

<sup>25</sup>V. Yu. Topolov and A. V. Turik, *Diffus. Defect Data, Pt. A* **123-124**, 31 (1995).

<sup>26</sup>J. Fousek and V. Janovec, *J. Appl. Phys.* **40**, 135 (1969); J. Sapiel, *Phys. Rev. B* **12**, 5128 (1975).

<sup>27</sup>V. Yu. Topolov, L. E. Balyunis, A. V. Turik, I. S. Bah, and O. E. Fesenko, *Izv. Ross. Akad. Nauk, Ser. Fiz.* **56**, 127 (1992); V. Yu. Topolov, L. E. Balyunis, A. V. Turik, I. S. Bah, and O. E. Fesenko, *Bull. Russ. Acad. Sci. Phys.* **56**, 1588 (1992).

<sup>28</sup>Y. U. Wang, *Phys. Rev. B* **73**, 014113 (2006).

<sup>29</sup>N. A. Pertsev and E. K. H. Salje, *Phys. Rev. B* **61**, 902 (2000).

<sup>30</sup>V. Yu. Topolov, *Fiz. Tverd. Tela (Leningrad)* **48**, 1260 (2006); V. Yu. Topolov, *Phys. Solid State* **48**, 1334 (2006).

<sup>31</sup>L. E. Balyunis, V. Yu. Topolov, A. V. Turik, and O. E. Fesenko, *Kristallografiya* **35**, 98 (1990) (in Russian).